

RESEARCH ARTICLE | MAY 22 2023

Low-frequency noise in Au-decorated graphene–Si Schottky barrier diode at selected ambient gases

J. Smulko ; K. Drozdowska; A. Rehman; ... et. al

 Check for updates

Appl. Phys. Lett. 122, 211901 (2023)

<https://doi.org/10.1063/5.0152456>


View
Online


Export
Citation

CrossMark



Time to get excited.
Lock-in Amplifiers – from DC to 8.5 GHz

[Find out more](#)

 Zurich
Instruments

Low-frequency noise in Au-decorated graphene-Si Schottky barrier diode at selected ambient gases

Cite as: Appl. Phys. Lett. **122**, 211901 (2023); doi: [10.1063/5.0152456](https://doi.org/10.1063/5.0152456)

Submitted: 30 March 2023 · Accepted: 9 May 2023 ·

Published Online: 22 May 2023



View Online



Export Citation



CrossMark

J. Smulko,^{1,a)} K. Drozdowska,¹ A. Rehman,² T. Welearegay,³ L. Österlund,³ S. Rummyantsev,² G. Cywiński,² B. Stonio,^{2,4} A. Krajewska,² M. Filipiak,^{2,4} and P. Sai²

AFFILIATIONS

¹Department of Metrology and Optoelectronics, Faculty of Electronics, Telecommunications, and Informatics, Gdańsk University of Technology, G. Narutowicza 11/12, 80-233 Gdańsk, Poland

²CENTERA Laboratories, Institute of High Pressure Physics PAS, Sokołowska 29/37, 01-142 Warsaw, Poland

³Department of Materials Science and Engineering, The Angstrom Laboratory, Uppsala University, P.O. Box 35, SE-75103 Uppsala, Sweden

⁴Centre for Advanced Materials and Technologies CEZAMAT, Warsaw University of Technology, Poleczki 19, 02-822 Warsaw, Poland

Note: This paper is part of the APL Special Collection on Electronic Noise: From Advanced Materials to Quantum Technologies.

^{a)}Author to whom correspondence should be addressed: janusz.smulko@pg.edu.pl

ABSTRACT

We report results of the current–voltage characteristics and low-frequency noise in Au nanoparticle (AuNP)-decorated graphene-Si Schottky barrier diodes. Measurements were conducted in ambient air with addition of either of two organic vapors, tetrahydrofuran [(CH₂)₄O; THF] and chloroform (CHCl₃), as also during yellow light illumination (592 nm), close to the measured particle plasmon polariton frequency of the Au nanoparticle layer. We observed a shift of the DC characteristics at forward voltages (forward resistance region) when tetrahydrofuran vapor was admitted (in a Au-decorated graphene-Si Schottky diode), and a tiny shift under yellow irradiation when chloroform was added (in not decorated graphene-Si Schottky diode). Significantly larger difference in the low-frequency noise was observed for the two gases during yellow light irradiation, compared with no illumination. The noise intensity was suppressed by AuNPs when compared with noise in graphene-Si Schottky diode without an AuNP layer. We conclude that flicker noise generated in the investigated Au-decorated Schottky diodes can be utilized for gas detection.

© 2023 Author(s). All article content, except where otherwise noted, is licensed under a Creative Commons Attribution (CC BY) license (<http://creativecommons.org/licenses/by/4.0/>). <https://doi.org/10.1063/5.0152456>

Due to numerous industrial and medical applications, better gas sensors are highly demanded. Two-dimensional materials (e.g., graphene, MoS₂, ZrS₃) are highly explored candidates for gas sensing areas because of the high ratio of the active surface to its volume. Low selectivity, limited sensitivity, and poor long-term stability are, however, challenges that must be met for any new material for gas sensing. More than two decades ago, it was proposed to utilize low-frequency (1/f-like) noise in resistive gas sensors for sensing applications, and it was denoted fluctuation-enhanced sensing (FES).^{1,2} The same method was subsequently applied on graphene back-gated field effect transistors (GFETs) and carbon nanotubes.^{3–5}

Low-dimensional materials have attracted large attention and reporting results suggesting high gas sensitivity.^{6–10} These materials (e.g., graphene layer) can operate as a channel in the back-gated field effect transistor. It was shown that the FES method could detect low

concentrations of organic vapors by observing Lorentzians in the 1/f-like spectrum in GFET of various graphene active areas.^{4,11}

In this study, we utilize the FES method for gas sensing in Schottky diodes consisting of p–n junctions between the graphene layer of quasi-metallic properties and n-doped silicon [Fig. 1(a)]. Such Schottky diodes have previously been applied for gas sensing.¹² Low-frequency noise in Schottky diodes have also been thoroughly studied and recorded in similar structures.^{13,14} This motivates us to apply the FES method on graphene-Si Schottky barrier diodes. Moreover, by decorating the graphene layer with Au nanoparticles (NPs), the catalytic and plasmonic effects on the gas sensing are investigated. It was previously reported that both graphene functionalization and AuNPs sputtered on the ZnO nanoparticles reduced sensor flicker noise.^{15,16} The noise reduction in AuNP/ZnO heterojunction structures may be attributed to the effect of localized surface plasmon resonances

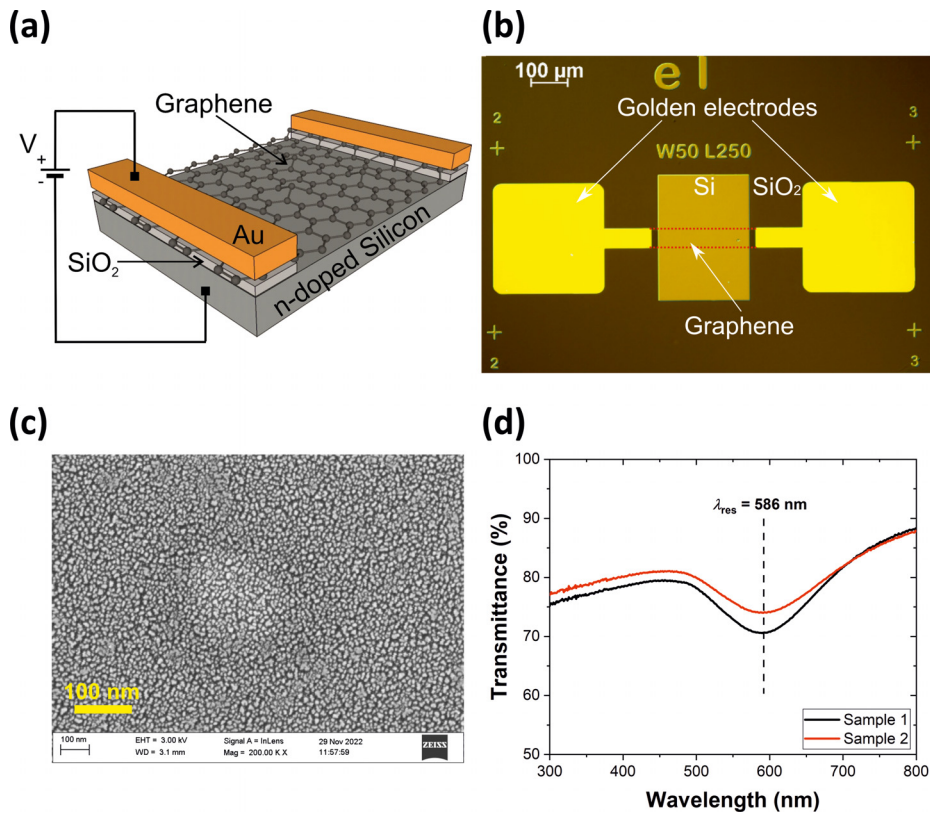


FIG. 1. (a) Schematic of a studied Schottky diode with the bias voltage source. (b) Optical microscopy image of a fabricated device before Au nanoparticle deposition with graphene dimensions: width = 50 μm, length = 250 μm. (c) Scanning electron microscopy (SEM) image of Au nanoparticles deposited on silicon substrate using AGD. The mean diameter of nanostructures is approximately 8 nm. (d) UV-vis spectra of two samples (Au nanoparticles deposited on glass substrates during the same AGD process) showing the local minimum transmittance at 586 nm corresponding to localized surface plasmon resonance (LSPR) exhibited by Au nanoparticles.

(LSPR), and the same effect may be anticipated in graphene decorated by AuNPs. We can also expect the presence of strong light–matter interactions in such graphene heterostructures, resulting in a light-modulated FES method for gas sensing, as suggested elsewhere.¹⁷

The graphene–Si Schottky diodes were prepared as follows. An n-type silicon wafer was cleaned and thermal oxidized to yield a targeted SiO₂ thickness of 90 nm. The SiO₂ thickness was confirmed by ellipsometry measurements. Afterward, the SiO₂ layer was selectively etched, and graphene was transferred to the Si/SiO₂ substrate via an electrochemical delamination process as described elsewhere.¹⁸ The graphene was grown on Cu foil via the CVD synthesis method and was bought from Graphenea company (<https://www.graphenea.com/>). It is a single layer of graphene with a theoretical thickness of 0.345 nm. Subsequently, graphene was patterned and selectively etched in oxygen plasma by reactive-ion etching (RIE). Finally, a thermal evaporator was employed to deposit Ni/Au (10/200 nm) contact electrodes for electrical characterizations of the fabricated devices. All of the lithography processes were performed by electron-beam lithography (JBX-9300FX). An optical microscopy image of the final graphene–Si Schottky device is shown in Fig. 1(b).

Gold nanoparticles were fabricated and deposited onto the graphene layer employing the Advanced Gas Deposition (AGD) technique, also referred to as “gas evaporation,”^{19,20} using an Ultra Fine Particle Equipment (ULVAC Ltd, Japan). Briefly, in AGD, metal nanoparticles are produced from their pure metal precursor in a source vacuum chamber by controlled melting of the metal and

cooling the ejected metal atoms by a gas (typically He) to form log-normally distributed nuclei. The particles are sucked into an upper deposition chamber held at lower vacuum through a stainless steel transfer pipe position with one end positioned close to the vapor zone above the Au melting point. The AuNPs are deposited on a substrate mounted on a programmable XY-stage, producing well-dispersed layers or log-normally size-selected, dispersed, non-contacting nanoparticles.²¹ In our case, a piece of high-purity Au (purity 99.99%) was placed in a graphite crucible positioned in the axial center of an RF copper coil in the source chamber.

By applying 2.8 kW to the coil, ultrapure Au nanoparticles were formed in a laminar flow of 20 l/min of He gas (purity 99.997%). Dispersed AuNPs were patterned on the graphene–Si devices over predefined substrate areas while moving at a rate of 2.5 mm/s. The AuNPs were prepared with pressures of 87 and 0.6 mbar in the lower evaporation chamber and an upper chamber, respectively. Before the fabrication and deposition of the nanoparticles, the two chambers were evacuated to 3×10^{-2} mbar.

Figure 1(c) shows a scanning electron microscopy (SEM) image of AuNPs on a Si substrate employing a Zeiss LEO 1550 instrument. The AuNPs are highly dispersed and uniformly distributed with a mean diameter of 8 ± 2 nm and were deposited on 0.5 mm thick quartz substrates for spectrophotometric characterization using a Perkin-Elmer Lambda 900 spectrophotometer. The AuNPs coverage is below one layer thickness.²¹ Figure 1(d) depicts the transmittance spectrum for monodispersed AuNPs prepared by AGD on glass.

The minimum of optical transparency corresponds to localized surface plasmon resonance (LSPR) of the AuNPs corresponding to a wavelength of about 586 nm (yellow light).

A probe station was used to establish the contacts to the investigated structures [Fig. 2(a)]. A gas distribution system (mass flow meters, type Analyt MTC GFC17) provided controlled vapors concentration by flowing synthetic air through a glass bubbler with the organic solvent [(CH₂)₄O or CHCl₃]. Keithley 4200-SCS setup within the bias voltage range between -4 and 4 V was employed to measure the current–voltage characteristics of the device. Yellow light irradiation (592 nm, type LED8-YD30) induced visible change in DC characteristic at reverse bias, increasing the Au-decorated graphene–Si DC response by about one order magnitude. The recorded change was independent of the ambient atmosphere. This effect can be explained by an induced photo-current in the n-doped silicon when the device is irradiated by yellow light. The generated photo-current is large enough not to be masked by thermal fluctuations, or adsorption-desorption events occurring at the exposed graphene interface. A shift of the DC characteristics occurred only when a forward bias voltage was applied in THF gas mixed in synthetic air (S.A.), when the diode equivalent serial resistance limited the forward current [e.g., at voltages larger than ~ 1.5 V, see Fig. 2(c)]. Two organic gases were selected (THF, chloroform) to investigate Schottky diode response to ambient gases. THF was selected because it is a Lewis base. Chloroform has hard acid-like chemical properties. These gases have different affinities for electrons. Apart from this, we suppose that there is an experimental reason for this selection, both having high vapor pressure (about 250 and 300 mbar at RT). The relative change $\Delta = (I_{\text{THF}} - I_{\text{S.A.}})/I_{\text{S.A.}}$ of

current at an ambient atmosphere of THF (I_{THF}) and an ambient atmosphere of synthetic air ($I_{\text{S.A.}}$) is about 10% and is seen to be slightly higher when the diode was irradiated with yellow light [Fig. 2(c)]. The same experiment was conducted for the graphene–Si Schottky diode, without AuNPs decoration, but with greater graphene area (width: $250 \mu\text{m}$, length: $250 \mu\text{m}$). In contrast to THF, we observed a tiny shift of DC characteristic in chloroform [Fig. 2(d)].

The current–voltage characteristic of the Schottky diode is given by the Shockley equation,

$$I = I_S \left[\exp\left(\frac{V}{\eta V_T}\right) - 1 \right], \quad (1)$$

where I_S represents saturation current at reverse bias, $V_T = k_B T/q$ is the thermal voltage (q —electron charge, k_B —Boltzmann constant, T —temperature [K]), η is the ideality factor, representing a slower rate of current increase than modeled in the ideal Schottky diode. Thus, the observed tiny shift of DC characteristic can be related to the change in the quasi-Fermi levels of the electrons and holes across the junction THF and chloroform, respectively, due to THF being a Lewis base and chloroform acting like a hard acid, but this effect requires further in-depth investigations. From the I–V characteristics in Fig. 2(c), represented in a log-linear scale, we calculate $\eta V_T = 0.17$ V.

The real diode has some series resistance that makes the diode characteristic Ohmic at higher bias voltages. The observed change in the parameter Δ in the DC characteristic in THF gas [Fig. 2(c)] can be explained by the diode series resistance increase due to the adsorbed THF molecules to the graphene layer, but also change in ideality factor may contribute. The Schottky junction is formed between the

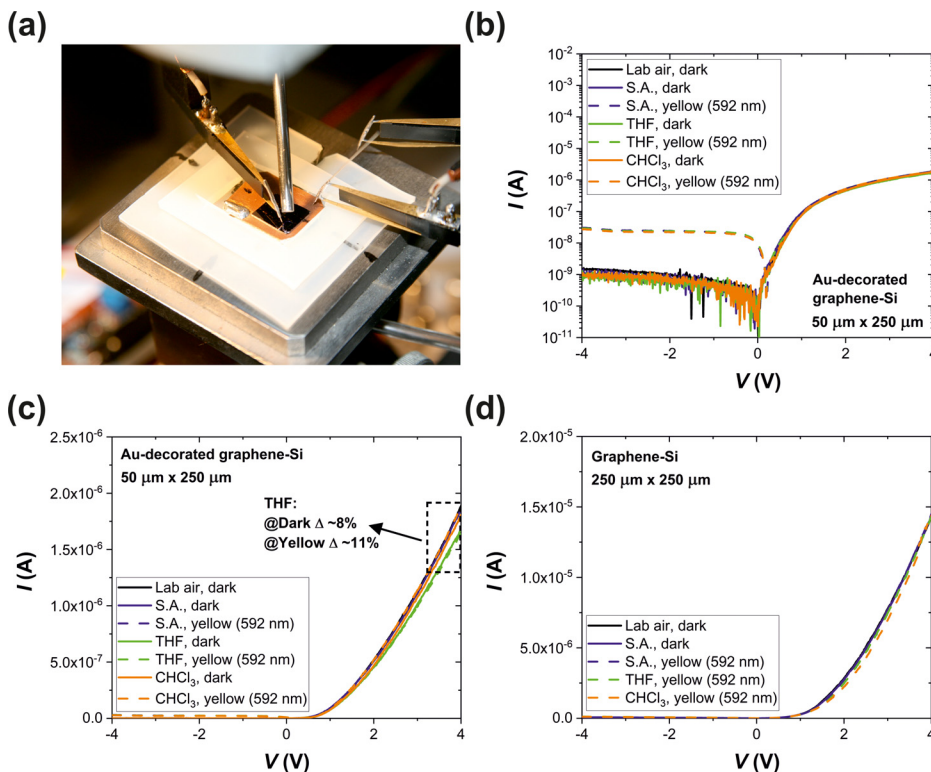


FIG. 2. (a) A probe station establishes two contacts by titanium needles to the diode structure and delivers gas through a metal pipe. The Keithley 4200-SCS setup recorded the DC characteristics. (b) Current–voltage characteristics (I–V) of Au-decorated graphene–Si Schottky diode in the dark and under yellow irradiation (592 nm; LED type), and in selected gases represented in logarithmic scale, and (c) in linear scale showing the changes for tetrahydrofuran (THF) in forward bias region. (d) I–V characteristics for graphene–Si diode without Au nanoparticles as a reference. The target gases were diluted in synthetic air (S.A.) to reach a concentration of 100 ppm for both gases.

graphene layer and n-doped silicon. A part of the graphene layer between the Au-contact electrode and the formed Schottky junction works as a series resistance for the diode, and any adsorbed molecules there can change its resistance. It is worth mentioning that the current between the graphene layer and n-doped Silicon is limited to a narrow path when their contact is established, as discussed in the literature.²² It means that the sensing area is even smaller than the applied dimensions of the graphene layer [Fig. 1(b)].

The low-frequency noise of the Schottky diodes was also measured. Low-frequency voltage fluctuations $u(t)$ were recorded by the NI USB-4431 data acquisition board over almost four frequency decades [Fig. 3(a)]. A battery biased the device under test to reduce power supply interferences. Low-noise voltage amplifier, Stanford SR760, gained 10^3 V/V times the voltage fluctuations measured across the Schottky diode. The power spectral density of voltage noise generated in the diode at different forward bias voltages is shown in Fig. 3(b). The power spectral density of the voltage fluctuations $S_V(f)$ is found to be proportional to the square of the bias voltage, V^2 , as shown in Fig. 3(c) for frequency $f_0 = 1$ Hz. The same dependence was observed for the investigated Au-decorated graphene-Si Schottky diode in the dark and under yellow light irradiation. It means that the recorded noise is generated by the Schottky diode in the measurement setup. There was a tiny difference in noise intensity when measured in the dark and yellow light irradiation. When we observed flicker noise in the graphene-Si Schottky diode, there was no difference in the noise intensity in the dark or under yellow irradiation [Fig. 3(d)]. Moreover, the graphene-Si Schottky diode exhibited more intense noise when

compared with the results observed for Au-decorated graphene-Si Schottky diode at selected bias voltage; e.g., at $V = 3.64$ V and $f_0 = 1$ Hz voltage power spectral density equals $S_V(f_0) = 2 \times 10^{-7}$ V²/Hz for Au-decorated and $S_V(f_0) = 3 \times 10^{-6}$ V²/Hz for the non-Au-decorated diode. The Au-decoration resulted in lower noise when compared with the non-decorated diode, even if the graphene-Si diode had a five times larger graphene area, which should result in lower $1/f$ noise intensity. The low-frequency noise suppression by Au nanoparticles has recently been reported for the AuZnO Schottky barrier when the AuNPs adsorbed some broadband emissions of deep-level defects into ZnO by localized surface plasmon resonance (LSPR).¹⁶ These emissions concentrated the electromagnetic field and resulted in more carriers excited by the LSPR. Thus, at a higher total number of excited charges, the relative fluctuations of the carrier's number were reduced, thus reducing $1/f$ noise.

The results of gas detection by the FES method in Au-decorated graphene-Si Schottky diodes are presented in Fig. 4. The power spectral densities $S_R(f)$ of resistance fluctuations were normalized to the square of serial resistance $(R_{S,diff})^2 = (dV/dI|_{V=3.64V})^2$, defined as a dynamic resistance (differential) of the voltage-current characteristic at a bias voltage $V = 3.64$ V. The recorded voltage fluctuations $u(t)$ were transformed to resistance fluctuations $R_S(t)$ of the Schottky diode to estimate its power spectral density $S_R(f)$ normalized to the square of the dynamic resistance $(R_{S,diff})^2$. The normalization makes the presented results independent of applied measurement setup and bias conditions. Following suggested methods in the literature,²³ we linearize the Schottky diode at the applied bias point and replace the diode

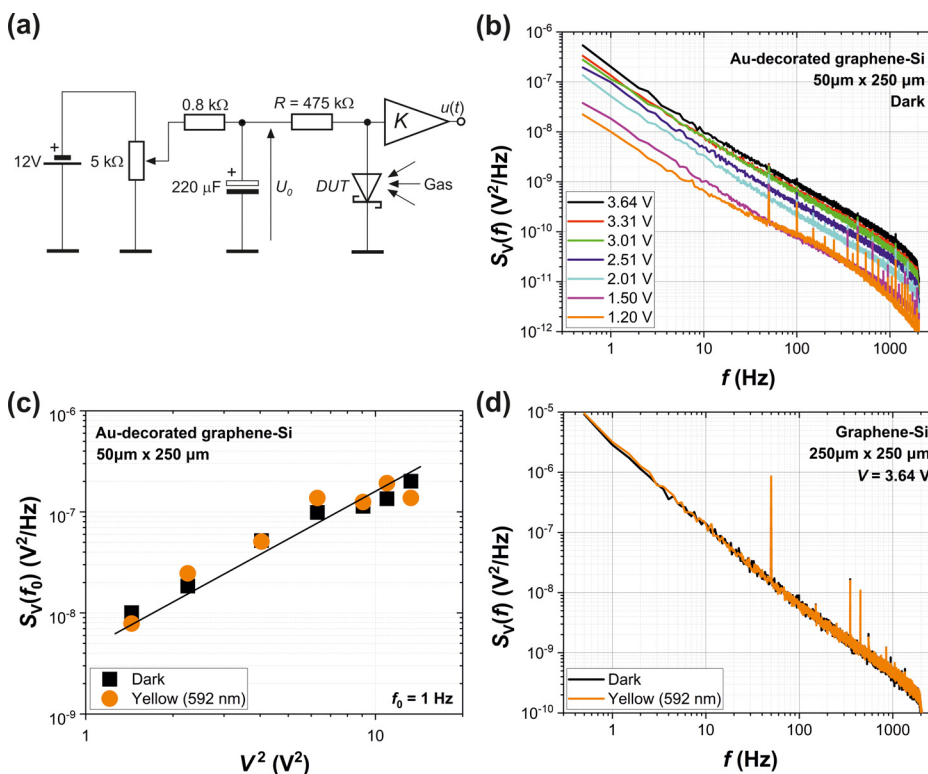


FIG. 3. (a) Schematic of the bias circuit used to measure current noise in Schottky diodes by low-noise voltage amplifier (Stanford, model SR760, voltage gain $K = 1000$ V/V) and data acquisition board (National Instruments, type USB-4431). (b) Power spectral density of voltage noise $S_V(f)$ generated in the Au-decorated graphene-Si Schottky diode under forward bias (1.20–3.64 V) in the dark. (c) Power spectral density of voltage noise $S_V(f_0)$ at frequency $f_0 = 1$ Hz vs bias voltage V across the diode, showing linear dependence as a function of V^2 in the dark and yellow light irradiation (592 nm, type LED8-YD30). (d) Power spectral density of voltage noise $S_V(f)$ generated in the graphene-Si Schottky diode under forward bias voltage of 3.64 V in the dark and yellow light irradiation, confirming no effect of irradiation on noise characteristics when the diode was not decorated by Au nanoparticles. All measurements were done in ambient conditions at room temperature.

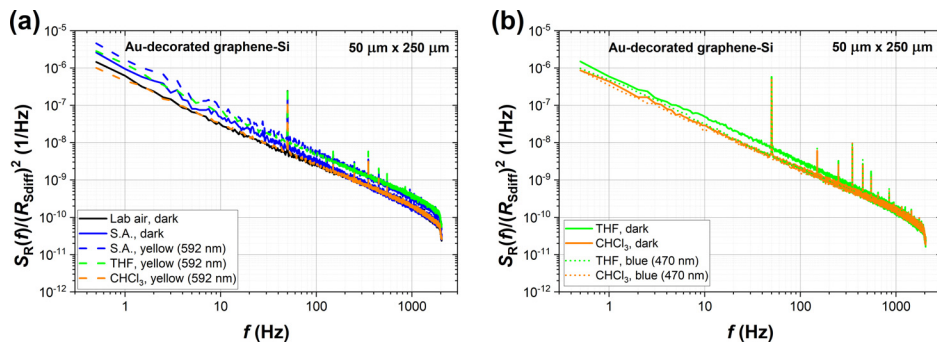


FIG. 4. Power spectral density of resistance fluctuations $S_R(f)$ normalized to the square of dynamic resistance R_{Sdiff}^2 for a forward biased Au-decorated graphene–Si Schottky diode at voltage bias $V = 3.64$ V in selected gases (laboratory air, synthetic air—S.A., tetrahydrofuran—THF, chloroform— $CHCl_3$): (a) in the dark and under yellow light irradiation (592 nm, type LED8-YD30), (b) in the dark and under blue light irradiation (470 nm, type LEDU-5BW25-F).

with the voltage source V_T and serial resistor R_{Sdiff} . The relationship between applied DC voltage U_0 [Fig. 3(d)] and voltage V_S across the resistance R_{Sdiff} then becomes

$$V_S = (U_0 - \eta V_T) \frac{R_{Sdiff}}{R + R_{Sdiff}}. \quad (2)$$

After that we define the parameter ε representing the rate of change of V_S as a function of R_{Sdiff}

$$\varepsilon = \frac{dV_S}{dR_{Sdiff}} = (U_0 - \eta V_T) \frac{R}{(R + R_{Sdiff})^2}. \quad (3)$$

The same Eqs. (2) and (3), but for linear resistors, were published earlier.²³ We can determine the relation between $S_R(f)$ and the measured $S_V(f)$ by considering the mean square resistance fluctuations in an infinitesimally small df bandwidth,

$$S_R(f)df = d\langle R_{Sdiff}^2(f) \rangle = \frac{d\langle V_S^2(f) \rangle}{\varepsilon^2} = \frac{S_V(f)}{\varepsilon^2} df, \quad (4)$$

and introducing Eq. (3) into (4), we get the formula to estimate the normalized power spectrum density of resistance fluctuations

$$\frac{S_R(f)}{R_{Sdiff}^2} = \frac{S_V(f)}{(U_0 - \eta V_T)^2} \left[\frac{(R + R_{Sdiff})^2}{R \cdot R_{Sdiff}} \right]^2. \quad (5)$$

The observed low-frequency noise in Fig. 4 follows $1/f$ frequency dependence. It suggests that the observed noise was generated mainly by mobility fluctuations, as reported elsewhere.²⁴ When the sample was irradiated by yellow light, we noticed differences in their intensity for selected gases. The $S_R(f)/(R_{Sdiff})^2$ value for THF was $1.67 \times 10^{-6} \text{ Hz}^{-1}$ at $f_0 = 1$ Hz [Fig. 4(a)], while it remained approximately the same for $CHCl_3$, yielding a difference in $S_R(f)/(R_{Sdiff})^2$ value by a factor of 2.8. When noise measurements were done in the dark, the difference between the spectra for THF and $CHCl_3$ was a factor of 1.2 at $f_0 = 1$ Hz [Fig. 4(b)]. The same noise measurements were then also performed under blue light irradiation (470 nm). The difference in noise intensities was similar to the results in the dark conditions (a factor of 1.4 at $f_0 = 1$ Hz). The results, thus, suggest that the FES method can be used for enhanced and selective LSPR gas sensing, yielding a factor of about three enhancement for THF—a known Lewis base (electron lone pair donor) molecule. The proposed hybrid structures and the FES method open new perspectives of advancing gas sensing by utilizing the LSPR phenomena easily modulated by LED light sources. The presented modulation and the FES method can improve gas

detection selectivity by reducing the number of gas sensors necessary to detect gas mixture components.^{25,26} The DC characteristics can also be applied to detect some gases. Moreover, such Schottky diode gas sensors operate at room temperature, and the modulating LED light source can be switched on quickly to secure low energy consumption.

In conclusion, we observed that the low-frequency noise in an Au-decorated graphene–Si Schottky barrier diode operating as a gas sensor can be applied for gas sensing by considering its power spectral intensity changes. The observed changes for two gas molecules with different chemical properties (tetrahydrofuran, being a Lewis base, and chloroform being a hard acid) were enhanced by a factor of about 2.8 times when the sensor was irradiated by yellow light. The effect is attributed to LSPR phenomena. In dark, or under blue light irradiation, the changes were similar and were small (<1.4 times). We suppose that this effect can be increased optimizing the parameters of Au decoration (e.g., size of AuNPs and its surface coverage density), as well as illumination conditions. Moreover, the studied Schottky diode did not exhibit drift over several weeks when stored in laboratory air. It means that the FES method can identify at least some organic solvents in feasible and practical conditions. It is worth mentioning that even more intense noise change was observed in gas sensor comprising of organically functionalized AuNPs when exposed to formaldehyde.²⁷ It suggests that the FES method applied in gas sensors utilizing AuNPs is worth of in-depth investigation.

The work was supported by the National Science Centre, Poland, the research project: No. 2019/35/B/ST7/02370, “System of gas detection by two-dimensional materials.” This study was also partially supported by CENTERA Laboratories in the frame of the International Research Agendas program for the Foundation for Polish Sciences, cofinanced by the European Union under the European Regional Development Fund (No. MAB/2018/9), and the H2020-MSCA-RISE project “Canleish” (Grant No. 101007653).

AUTHOR DECLARATIONS

Conflict of Interest

The authors have no conflicts to disclose.

Author Contributions

Janusz Smulko: Conceptualization (equal); Supervision (lead); Visualization (equal); Writing – review & editing (equal). **Maciej Filipiak:** Resources (equal). **Pavlo Sai:** Resources (equal). **Katarzyna Drozdowska:** Data curation (lead); Investigation (lead); Visualization

(equal). **Adil Rehman**: Data curation (supporting); Resources (equal); Writing – review & editing (supporting). **Tesfalem Welearegay**: Resources (equal); Visualization (equal); Writing – review & editing (equal). **Lars Österlund**: Conceptualization (equal); Visualization (equal); Writing – review & editing (equal). **Sergey L. Rumyantsev**: Conceptualization (equal); Writing – review & editing (equal). **Grzegorz Cywiński**: Writing – review & editing (equal). **Bartłomiej Stonio**: Resources (equal). **Aleksandra Krajewska**: Resources (equal).

DATA AVAILABILITY

The data that support the findings of this study are available from the corresponding author upon reasonable request.

REFERENCES

- ¹L. B. Kish, R. Vajtai, and C. G. Granqvist, “Extracting information from noise spectra of chemical sensors: Single sensor electronic noses and tongues,” *Sens. Actuators, B* **71**(1–2), 55 (2000).
- ²A. Dziedzic, A. Kolek, and B. Licznarski, “Noise and nonlinearity of gas sensors—preliminary results,” in Proceedings of 22nd International Spring Seminar on Electronics Technology, 1999.
- ³S. Rumyantsev, G. Liu, M. S. Shur, R. Potyrailo, and A. A. Balandin, “Selective gas sensing with a single pristine graphene transistor,” *Nano Lett.* **12**(5), 2294 (2012).
- ⁴A. A. Balandin, “Low-frequency $1/f$ noise in graphene devices,” *Nat. Nanotechnol.* **8**(8), 549 (2013).
- ⁵K. Drozdowska, A. Rehman, A. Krajewska, D. V. Lioubtchenko, K. Pavlov, S. Rumyantsev, J. Smulko, and G. Cywiński, “Effects of UV light irradiation on fluctuation enhanced gas sensing by carbon nanotube networks,” *Sens. Actuators, B* **352**, 131069 (2022).
- ⁶E. Llobet, “Gas sensors using carbon nanomaterials: A review,” *Sens. Actuators, B* **179**, 32 (2013).
- ⁷S. Yang, C. Jiang, and S. Wei, “Gas sensing in 2D materials,” *Appl. Phys. Rev.* **4**(2), 021304 (2017).
- ⁸M. Donarelli and L. Ottaviano, “2D materials for gas sensing applications: A review on graphene oxide, MoS₂, WS₂, and phosphorene,” *Sensors* **18**(11), 3638 (2018).
- ⁹T. Li, W. Zeng, and Z. Wang, “Quasi-one-dimensional metal-oxide-based heterostructural gas-sensing materials: A review,” *Sens. Actuators, B* **221**, 1570 (2015).
- ¹⁰C. Anichini, W. Czepa, D. Pakulski, A. Aliprandi, A. Ciesielski, and P. Samorì, “Chemical sensing with 2D materials,” *Chem. Soc. Rev.* **47**(13), 4860 (2018).
- ¹¹K. Drozdowska, A. Rehman, P. Sai, B. Stonio, A. Krajewska, M. Dub, J. Kacperski, G. Cywiński, M. Haras, S. Rumyantsev, L. Österlund, J. Smulko, and A. Kwiatkowski, “Organic vapor sensing mechanisms by large-area graphene back-gated field-effect transistors under UV irradiation,” *ACS Sens.* **7**(10), 3094 (2022).
- ¹²A. Fattah and S. Khatami, “Selective H₂S gas sensing with a graphene/n-Si Schottky diode,” *IEEE Sens. J.* **14**(11), 4104 (2014).
- ¹³A. Kumar, R. Kashid, A. Ghosh, V. Kumar, and R. Singh, “Enhanced thermionic emission and low $1/f$ noise in exfoliated graphene/GaN Schottky barrier diode,” *ACS Appl. Mater. Interfaces* **8**(12), 8213 (2016).
- ¹⁴M. Zhu, X. Li, X. Li, X. Zang, Z. Zhen, D. Xie, and H. Zhu, “Schottky diode characteristics and $1/f$ noise of high sensitivity reduced graphene oxide/Si heterojunction photodetector,” *J. Appl. Phys.* **119**(12), 124303 (2016).
- ¹⁵B. Zhang, L. Qiao, and C. Tianhong, “Ultra-sensitive suspended graphene nanocomposite cancer sensors with strong suppression of electrical noise,” *Biosens. Bioelectron.* **31**(1), 105 (2012).
- ¹⁶I. B. Elkamel, N. Hamdaoui, A. Mezni, R. Ajjel, and L. Beji, “Effects of plasmon resonance on the low-frequency noise and optoelectronic properties of Au/Cu codoped ZnO based photodetectors,” *Opt. Quantum Electron.* **55**(2), 148 (2023).
- ¹⁷L. Britnell, R. M. Ribeiro, A. Eckmann, R. Jalil, B. D. Belle, A. Mishchenko, Y. J. Kim, R. V. Gorbachev, T. Georgiou, S. V. Morozov, A. N. Grigorenko, A. K. Geim, C. Casiraghi, A. H. Castro Neto, and K. S. Novoselov, “Strong light-matter interactions in heterostructures of atomically thin films,” *Science* **340**(6138), 1311 (2013).
- ¹⁸M. Dub, P. Sai, A. Przewłoka, A. Krajewska, M. Sakowicz, P. Prystawko, J. Kacperski, I. Pasternak, G. Cywiński, D. But, W. Knap, and S. Rumyantsev, “Graphene as a Schottky barrier contact to AlGaIn/GaN heterostructures,” *Materials* **13**(18), 4140 (2020).
- ¹⁹C. G. Granqvist and R. A. Buhrman, “Ultrafine metal particles,” *J. Appl. Phys.* **47**, 2200 (1976).
- ²⁰C. Hayashi, R. Uyeda, and A. Tasaki, *Ultra-Fine Particles: Exploratory Science and Technology* (Elsevier, 1997).
- ²¹T. F. Welearegay, U. Cindemir, L. Österlund, and R. Ionescu, “Fabrication and characterisation of ligand-functionalised ultrapure monodispersed metal nanoparticle nanoassemblies employing advanced gas deposition technique,” *Nanotechnol.* **29**(6), 065603 (2018).
- ²²D. K. Schroder, *Semiconductor Material and Device Characterization* (John Wiley & Sons, 2015).
- ²³B. Ayhan, C. Kwan, J. Zhou, L. B. Kish, K. D. Benkstein, P. H. Rogers, and S. Semancik, “Fluctuation enhanced sensing (FES) with a nanostructured, semiconducting metal oxide film for gas detection and classification,” *Sens. Actuators, B* **188**, 651 (2013).
- ²⁴A. Rehman, J. A. D. Notario, J. S. Sanchez, Y. M. Meziani, G. Cywiński, W. Knap, and S. Rumyantsev, “Nature of the $1/f$ noise in graphene—Direct evidence for the mobility fluctuation mechanism,” *Nanoscale* **14**(19), 7242 (2022).
- ²⁵H. C. Chang, L. B. Kish, M. D. King, and C. Kwan, “Fluctuation-enhanced sensing of bacterium odors,” *Sens. Actuators, B* **142**, 429 (2009).
- ²⁶J. W. Gardner and P. N. Bartlett, *Electronic Noses: Principles and Applications* (Oxford University Press, Oxford, UK, 1999).
- ²⁷L. Lentka, M. Kotarski, J. Smulko, U. Cindemir, Z. Topalian, C. G. Granqvist, R. Calavia, and R. Ionescu, “Fluctuation-enhanced sensing with organically functionalized gold nanoparticle gas sensors targeting biomedical applications,” *Talanta* **160**, 9–14 (2016).